SEMARAK ILMU PUBLISHING

Journal of Advanced Research in Applied Mechanics

Journal homepage:
https://semarakilmu.com.my/journals/index.php/appl_mech/index
ISSN: 2289-7895

Surface Post-Treatments of Different Lattice Structures Manufactured by 3D Printing using Selective Laser Melting

Moqdad J. Dakhil [1*], Abdulraheem Khadim AbidAli[1]

[1] Department of Metallurgical, College of Materials Engineering, University of Babylon, Babylon, Iraq

ARTICLE INFO

Article history:
Received 29 August 2024
Received in revised form 1 October 2024
Accepted 7 October 2024
Available online 30 October 2024

Keywords:
Additive manufacturing; Selective Laser Melting; Ti6Al4V alloys; Surface roughness; Electro polish

ABSTRACT

Selective laser melting (SLM) offers great potential for the fabrication of Ti6Al4V lattice structural components, but the resulting surface roughness of the manufactured products severely limits the use of the parts in biomedical applications. To reduce the influence of high surface roughness, the post processing process techniques applicable to all different lattice structures. In this study, two techniques were combined: ultrasonic abrasive flow and electro polishing treatment. To analyze Selective laser melted parts after post processing process, porosity and microstructural analyses were done. Furthermore, checking the influence of Electro polish time on surface of lattice structures. EP treatment conducted, applying a voltage of 20 ,18, and 16(V) And also (8), (6) and (4) minutes sequentially at a temperature of (4-7) C^o for HC, FCC, and BCC lattice structure specimens, sequentially. Acid-based electrolyte to perform Electro Polish, its solutions proved to be effective in reducing average surface roughness Ra from 7.325,7.465 and 6.7732.7 µm to 4.661 .3.911 and 4.20 for hexagonal, face center cubic and body center cubic lattice structures. In addition to, Rz from 36.766 ,35.768 and 30.029 to 22.482 ,17.88 and 18.249 µm sequentially. After post processing process, the findings of surface roughness, Young's modulus, yield strength, and Porosity percentage are compatible with the properties of bone, allowing it to be utilized as a scaffold.

1. Introduction

Additive manufacturing (AM) enables the creation of highly complex shapes that are difficult to achieve with conventional subtractive techniques. It offers unparalleled design freedom, supporting customization, rapid prototyping, and on-demand production. This technology also reduces material waste, lowers tooling costs, and shortens lead times. However, several challenges in AM still need to be addressed [1-3]. The limitations of AM, including the high threshold for achieving high precision and the issue of poor surface roughness, hinder further development [4,5] non-stochastic arrangements, known as lattice structures, are highly ordered. Full control over individual unit cells provides greater control over the structure's properties. [5]. Lattice structures

* *Corresponding author.*
E-mail address: mat.muqdad.jabur@uobabylon.edu.iq

https://doi.org/10.37934/aram.126.1.7997

are commonly utilized in lightweight design to minimize material waste and reduce energy consumption during the manufacturing process. By designing and optimizing lattice structures, significant savings in energy, materials, and manufacturing time can be achieved [6-8]. The increased adoption of lattice structures is attributed to the versatility of Additive Manufacturing (AM) techniques. This is particularly significant in biomedical applications where precision and customization are essential as shown in Figure 1 [9,10]. Examples include tissue engineering, orthopedic implants, and prosthetics [11]. AM's capability to create precise end parts tailored to human anatomy through lattice structures is particularly advantageous in biomedical fields like tissue engineering [12]. The ability to create lattice topologies with strut diameters spanning from submicron to millimeters enables the production of functional lattice structures tailored to specific applications and geometrical requirements. This is made feasible by advancements in manufacturing technology, particularly the emergence of Additive Manufacturing (AM) techniques like laser powder bed fusion manufacturing [13].

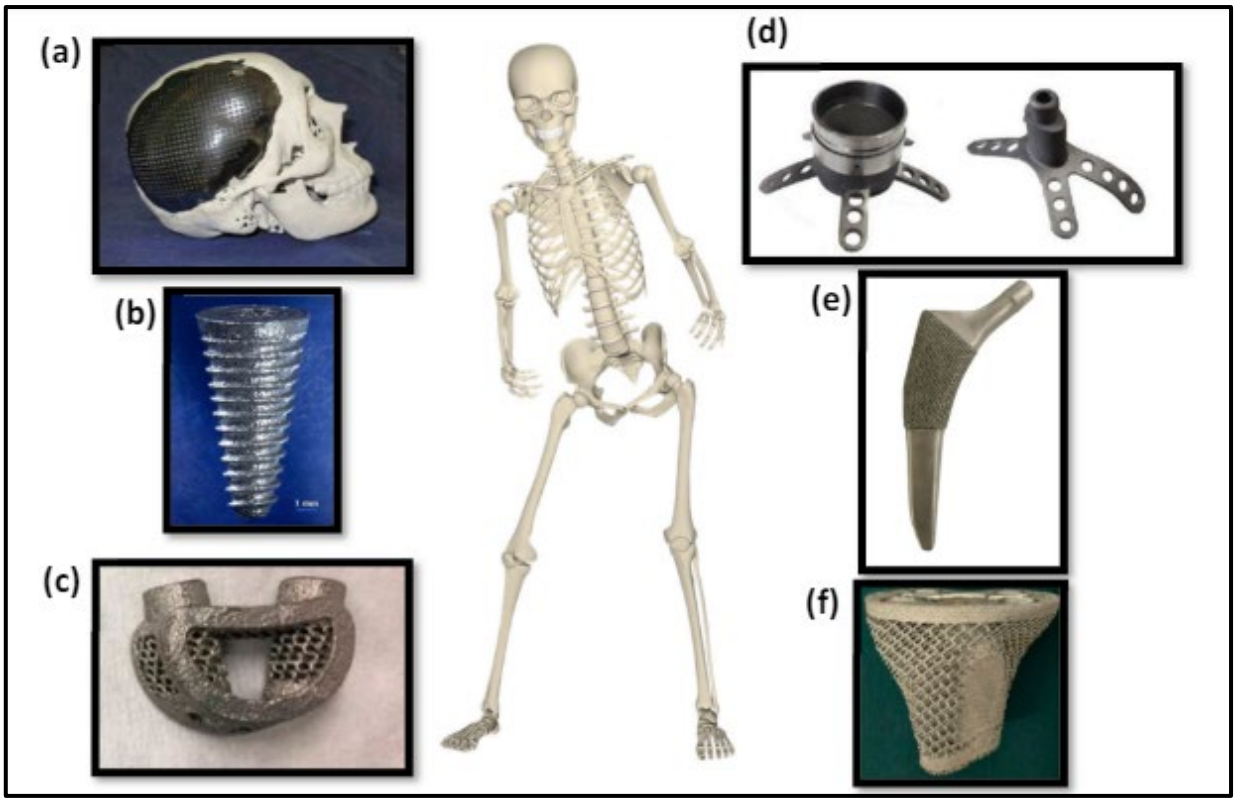

Fig. 1. illustrates the medical applications of 3D printing with metals, which include (a) cranial prostheses (b) dental implants (c) spinal cord implants (d) surgical guides (e) hip prostheses and (f) inter body fusion cages [14-17]

1.1 Laser Powder Bed Fusion

Selective Laser Melting (SLM) is generally acknowledged as a prominent metal AM technique for creating highly designed aeronautical, biomedical, and many other technical components [18,19]. The procedure uses a three-dimensional computer-aided design plan to generate two-dimensional cross-sectional slices of the model. A powder distribution device evenly spreads a fine coating of powder throughout the construction area. A high-intensity laser is utilized to specifically melt the specified areas of powder as indicated in the execution build file. These areas correspond to the successive layers of the computer-aided design (CAD) model. After each laser cycle, a fresh cross-

sectional slice of the item is produced. Then, the work platform is slowly lowered before the next layer of powder is added [20]. The SLM technique involves the controlled melting of individual layers of metal powder to form a particular component shape based on a predetermined pattern. However, flaws in AM structures may occur due to several physical phenomena that occur when the laser beam interacts with the powder bed. These factors involve the dynamics of the melted pool, the way powder particles adhere to each other, the process of certain components evaporating at high laser powers and slow speeds, and the creation of unstable phases in the material caused by fast cooling rates as shown in Figure 2 [21].

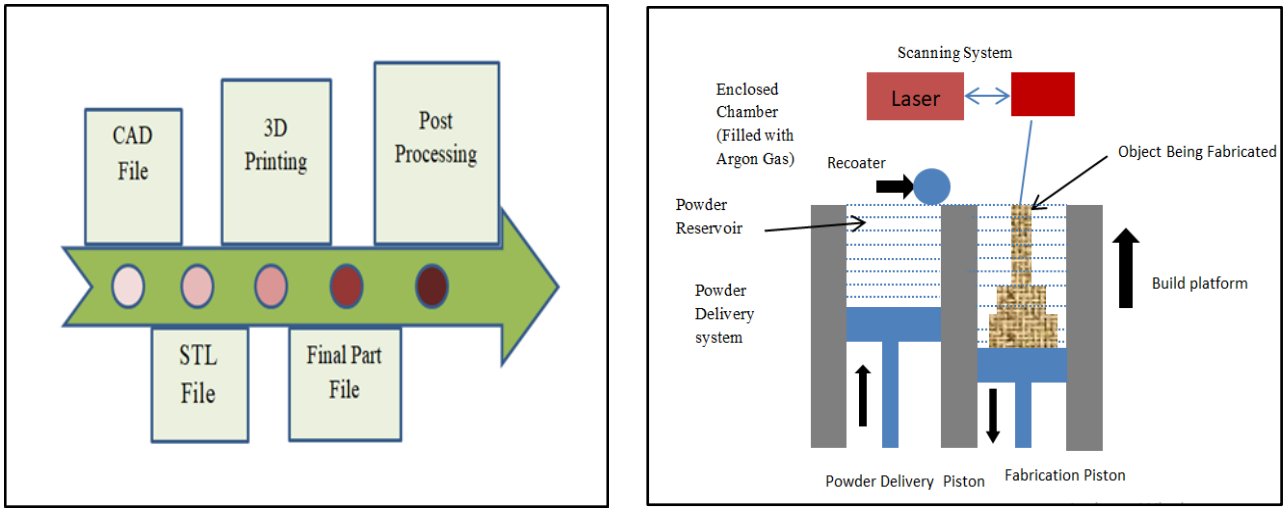

(a) (b)

Fig. 2. (a) Basic process of 3D printers to create 3D object (b) Schematic diagram for SLM technique

The geometric characteristics of the produced parts include agglomerated powder particles that are partially solidified near the melting pool, leading to undesired surface roughness on the scale of a few particle sizes [22]. It's important to acknowledge that the rough surface finish of these implants may promote bone growth compared to conventionally manufactured counterparts. This is due to the increased surface area available and the entrapment of cells in the free gaps between the particles [23]. In addition, the adverse influences of poor surface roughness and porosity defects during the AM process impact the resulting mechanical behavior, including elastic and plastic deformation. Therefore, it is imperative to address these defects to attain optimal performance from lattice structures [24,25]. Various post-processing techniques such as electro-polishing, laser surface modifications (such as re-melting and shock peening), mechanical surface finishing (including planar polishing and tumble polishing), and chemical polishing are typically necessary to enhance both the mechanical properties and surface quality [26].

Upon exploring various techniques, both individually and in combination, all techniques demonstrated decreases in surface roughness of the SLM parts. However, a common challenge with many of these techniques is their limited effectiveness in polishing complex-shaped parts. Electro-polishing (EP) emerges as a promising technique for polishing complex shapes [27-29]. In the study, Different patterns of lattice structures such as FCC, BCC, and HC were studied because it is possible to achieve mechanical properties and porosities that are comparable to those of human bone where help reducing stress shielding, integrating with the host bone. The hexagonal cubic model gives the possibility of increasing mechanical properties such as yield strength with a low modulus of elasticity which allow bony in-growth when used as an orthopedic scaffold.

1.2 Electro-Polishing Techniques

Electro-polishing stands out as a distinctly different technique from conventional finishing techniques, primarily because it is considered a non-contact machining process, ensuring damage-free treatment. The essence of electro-polishing lies in the removal of roughness without inducing crystallographic or grain-boundary alterations, resulting in the creation of bright and smooth surfaces [30]. EP involves an electrochemical mechanism where the corrosion of an anode, immersed in an electrolyte, is hastened by introducing an electric current into an electrolytic cell. Essential components of an electrolytic cell include an anode, a cathode, a power supply, and an electrolyte, facilitating the reaction [31-38].

During electrolysis, a current pass through the anode, cathode, and electrolyte, causing the anode to dissolve and the cathode to be plated. In an electrolytic cell, two simultaneous reactions occur: electro polishing of the anode and electroplating of the cathode. Fundamentally, material removal in electro-polishing involves the electrochemical dissolution of the work piece surface. Electrolysis operates based on Faraday's Law of electrolysis, which asserts that the amount of material (m) dissolved from the workpiece is directly proportional to the current (A) applied. Moreover, the quantity of material dissolved by a fixed amount of current is directly proportional to their respective chemical equivalent weights [30].

Various factors may impact the level of surface smoothness achieved with EP. These factors involve the applied potential or current density, temp, electrolyte kind, stirring rate, anode-cathode distance, anode's chemical makeup, and more variables. During the process, a thin layer of metallic oxide with a high specific gravity form covers the anode surfaces. The film displays different thicknesses across its surface, with the greatest thickness occurring over the valleys of micro-depressions and the smallest thickness over the peaks of micro-projections, as seen in Figure 3.

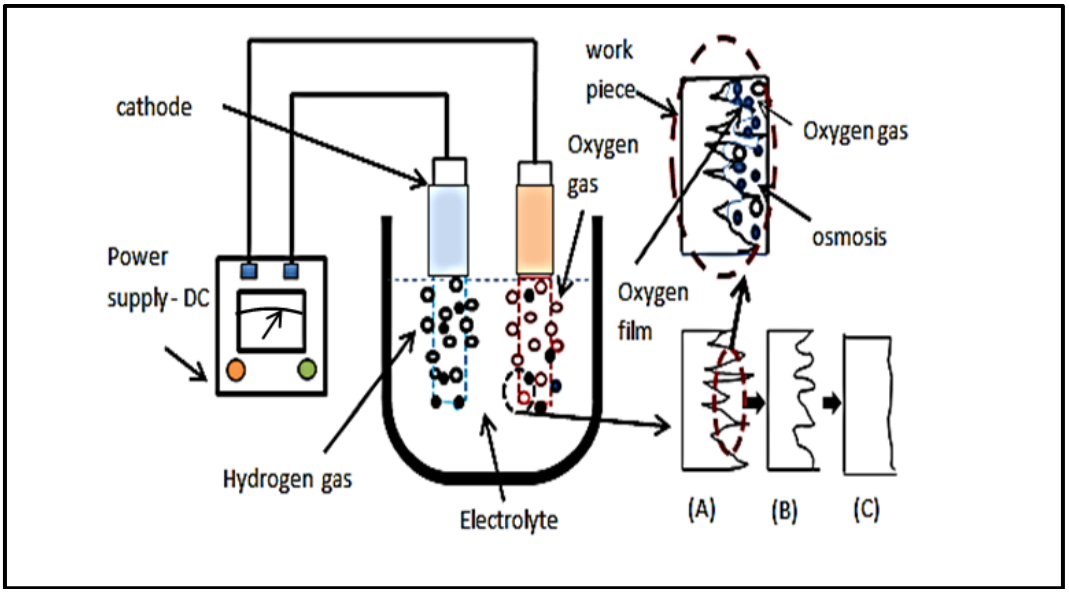

Fig. 3. Representation of the electrochemical polishing basic mechanism (a) Initial surface (b) On polishing surface and (c) Polished surface

2. Additive Manufacturing Process

All lattice structure specimens were fabricated utilizing SLM in an argon atmosphere. The SLM process was conducted on a Metal 3D printer (NOURA Company model M1OOP), equipped with a

300 W fiber laser having an 80 µm spot size and offering a building volume of Ø125 mm – 150 mm. Parameters for the SLM process included a layer thickness of 20-80 µm and a scanning speed of 7 m/s .The NOURA SLM software provides detailed information about the building process, including the positions of the building and powder platforms, the number of layers built and remaining, the remaining time, and other relevant data as shown in Figure 4. In this study, the scan direction was initially fused at a 45° angle to the horizontal line and then rotated by 90° for each new layer. The rotation patterns of 90°, 67.5°, and 45° involved counterclockwise rotation of the laser direction after each layer. Table 1 shown the process parameters for SLM utilized in specimen manufacturing. Energy density is the key process parameter that establishes the relationship between laser power, exposure velocity, hatching distance, and layer thickness. These parameters were selected based on previous research experience [39].

Table 1
Printing parameters used in the selective laser melting process

Laser power	240 (J)
Hatching distance	0.9 (mm)
Layer thickness	30(µm)
Energy density	88 (J/mm³)
Scan speed	1000 (mm/min)
focus diameter	Approx. 80 (µm)
Operating temperature	15-25 (C°)

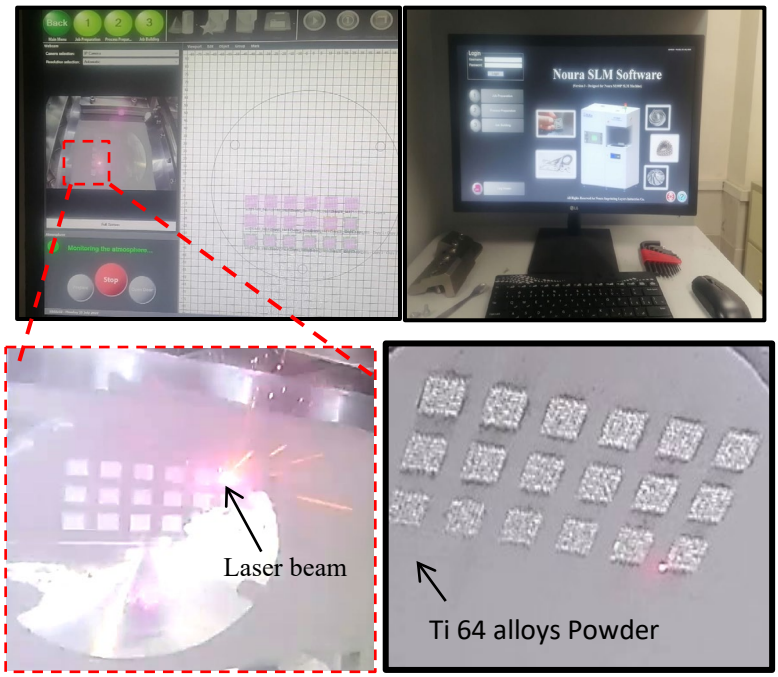

Fig. 4. Layer by layer building of the model by SLM

3. Material and Techniques

Powder particle analyses were performed utilizing a Better size 2000 laser particle size analyzer. The surface roughness was measured both before and after post-process treatment using a surface roughness tester. This device, a portable stylus-type profile meter, is the Mahr-PS1 unit manufactured by the Mahr Company in Germany.

The morphology of the lattice structures included face-centered cubic, body-centered cubic, and hexagonal cubic patterns. Specimens were fabricated with constant porosity ratios, and the porosity percentage was calculated utilizing Eq. (1), Where W1 is actual weight, W2 is the theoretical weight.

$$P\% = 1 - \frac{\mathrm{W1}}{\mathrm{W2}} * 100 \quad (1)$$

The lattice structures were designed with dimensions of (8×8×16) mm. For each manufactured part, mechanical testing to determine the elastic modulus and yield strength was conducted utilizing a computer-controlled Universal Testing Machine (200 kN). Specimens were tested at a constant displacement rate of 0.5 mm/min. The stress-strain curve was utilized to derive the elastic modulus and yield strength. Phase analysis has been conducted utilizing an XRD generator with a Cu target at a max tube voltage of 60 kV and a max tube current of 80 mA, with a scanning speed of 3° of 2θ per minute from 0º to 75º. Cu Kα radiation (λ = 1.5405 Å) was utilized for the XRD analysis. Figure 5 illustrates the XRD instrument (XRD-6000 Model, Shimadzu X-ray Diffractometer). The morphology of the 3D-printed lattice structures before and after post-processing was observed utilizing a scanning electron microscope (TESCAN, TYPE VEGA3, No.118-0014 SEM) at an accelerated voltage of 10 kV. Finally, electro polishing was employed as a finishing process to improve surface quality and remove unwanted powder. Acid-based electrolytes are commonly utilized to electro polish titanium and its alloys. An electrolyte composed of 640 ml/L of acetic acid, 200 ml/L of 60% perchloric acid, and 160 ml/L of 95% ethanol was utilized for electro polishing the lattice structure specimens. Various parameters affect the quality of the surface finish achieved by electro polishing. In this study, the potential (V) applied, the stirring rate, and the anode–cathode distance was optimized based on trial and error. The electrolyte was kept at about constant low temperature of (4-8)°C utilizing an ice bath. The electro polishing process was conducted with the lattice structure specimens as the anode, and type 304 stainless steel was utilized as the cathode.

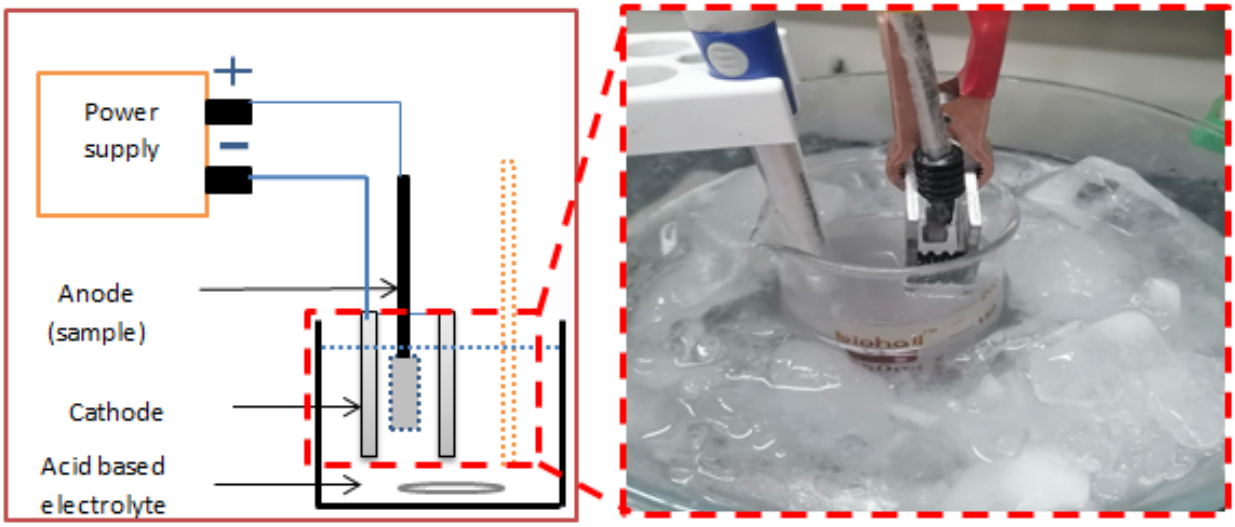

Fig. 5. Electro-Polish cell: lattice structure specimens as anode, 304 stainless steels as cathode

3.1 A powder Alloys

A powder of Ti-6Al-4V alloy made in (NOURA Company,), was utilized to prepare the lattice structure. The chemical composition of this powder alloy is shown in Table 2.

Table 2
Chemical composition analysis of the Powder Ti-6Al-4V alloys

Element%	Al	V	Fe	O	C	N	H	Y	Ti
ASTM B-348	5.5-6.75	3.5-4.5	0.4	0.2	0.08	0.05	0.015	-	remainder
Min.	5.5	3.5	-	-	-	-	-	-	remainder
Max.	6.75	4.50	0.30	0.20	0.08	0.05	0.015	0.005	remainder

3.2 Particle Size Analysis and Morphology of Powder

The powder particles' size distribution for the Powder Ti6Al-4V alloys cumulated mass had magnitudes as follows: D10 = 20.88 µm, D50 = 39.90 µm, D90 = 59.56 µm. Scanning electron microscopy (SEM) images of the powder grains, depicted in Figure 6, show that the particles are spherical or near spherical with smooth surfaces.

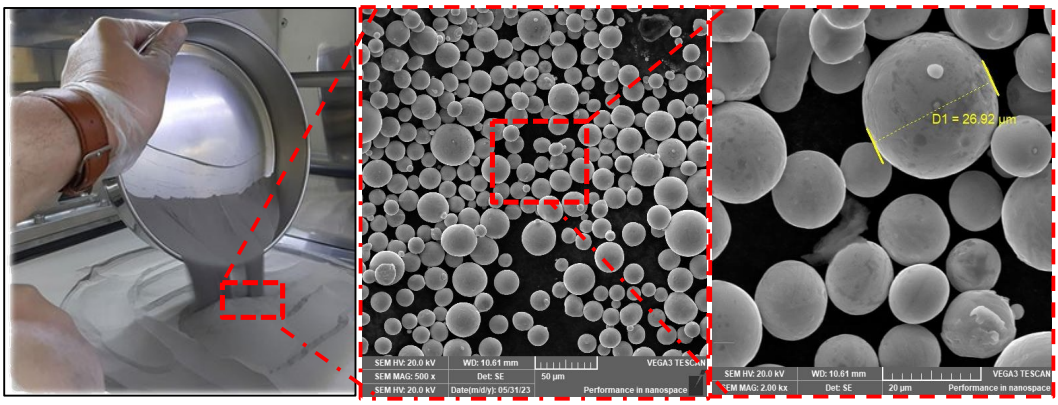

Fig. 6. The morphology of Ti6Al4V powder

3.3 X-ray Diffraction

The X-ray diffraction pattern of the Ti-6Al-4V alloy powder, shown in Figure 7, reveals the presence of a primary α-Ti (HCP) phase and a secondary β-Ti (BCC) phase. The X-ray diffraction analysis has been conducted to confirm the composition of the Ti6Al-4V powder alloy. The identified phases were matched against standard reference patterns for titanium from the powder file (JCPDS card No. 09-0432).

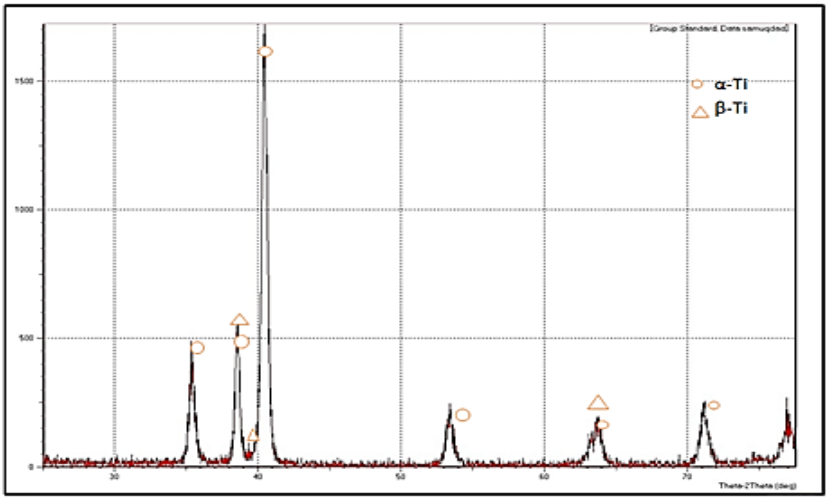

Fig. 7. XRD patterns of Ti-6Al-4V Powder

4. Results and Discussion

4.1 Ultrasonic abrasive (Sic) flows

During ultrasonic abrasive (SiC) flows, the residual powder such as unmolten particles and loosely bound particles clusters, it is in the under surface of the printed lattice's structure specimens as shown in Figure 8. For 20 minutes, we observe the residual powders suspend in the solution, after ultrasonic abrasive cleaning procedures, specimens were rinsed with DI water and cleaned in an ultrasonic bath as illustrated in Figure 9.

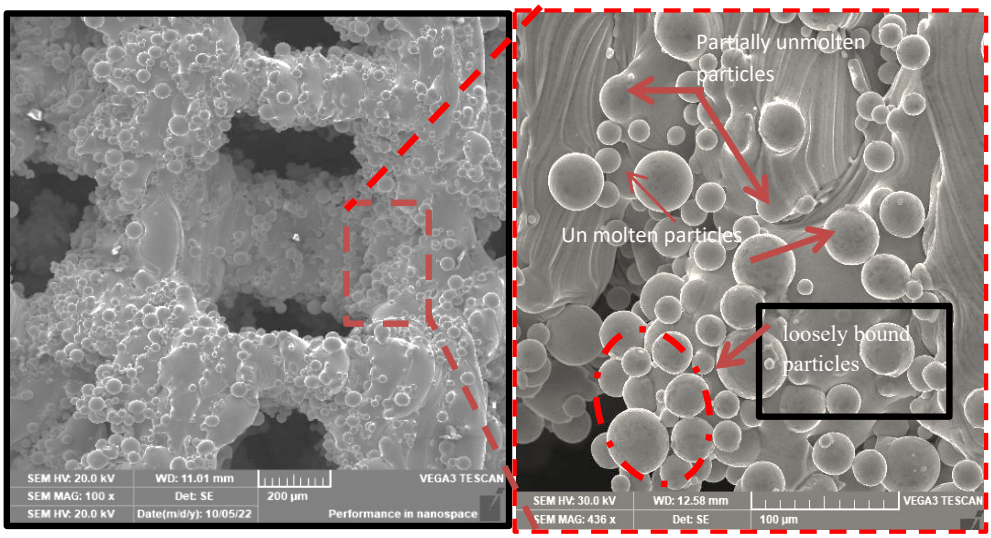

Fig. 8. SEM images of clusters of unmolten particles and loosely bound particles

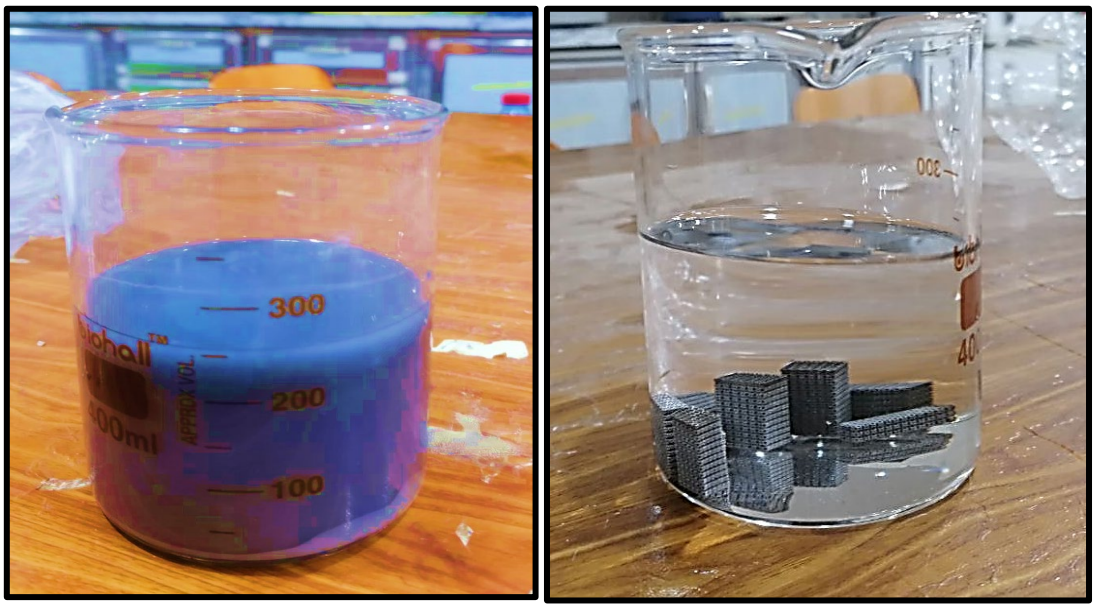

Fig. 9. (a) Residual powders suspended in the solution (b) Before ultrasonic Abrasive flow

4.2 Electro-polish treatment (EP)

The electro polish process condition was explored to identify optimal time magnitudes to reduce defects such as the attached partially melted particles and balling influence, it is resulting from the SLM process during building specimens. In the present study, the aim of EP treatment is

defects reducing defects without the influence on the mechanical and chemical properties for the different lattices structure (BCC, FCC and HC) specimens. EP treatment conducted, applying a voltage of 20, 18, and 16 (V) at a temperature of (4-8) C^{o} for HC, FCC, and BCC lattice structure specimens, sequentially as shown in Figures 10-12 respectively.

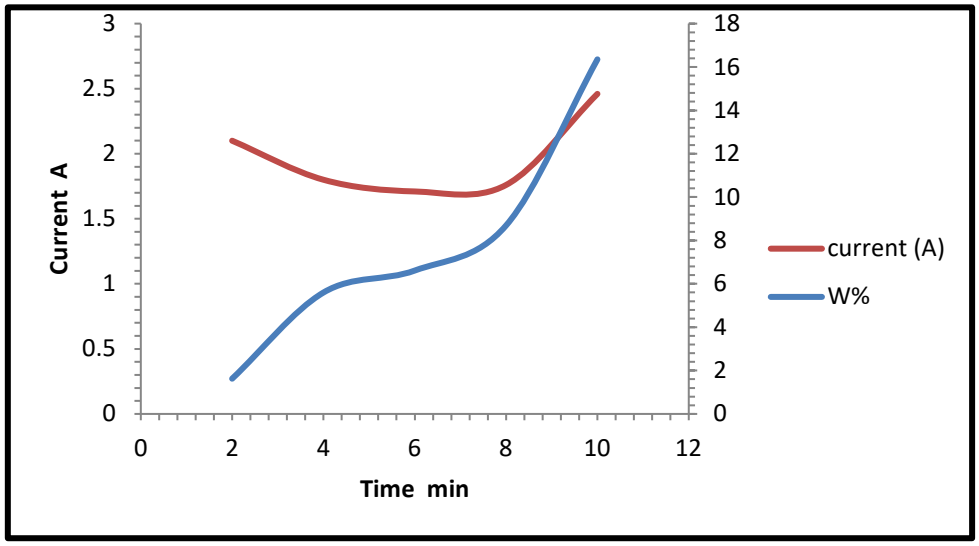

Fig. 10. Current (A) and weight loss percentage (%) versus different duration time for EP treatment at 20 V of HC specimen

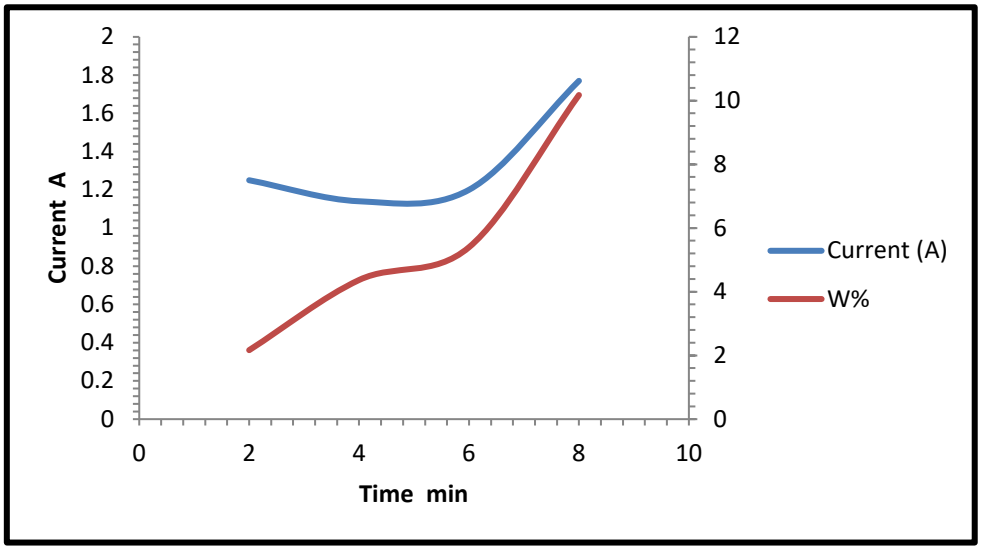

Fig. 11. Current(A) and Weight loss percentage (%) versus different duration time for Electro polishing treatment at 18V of FCC specimens

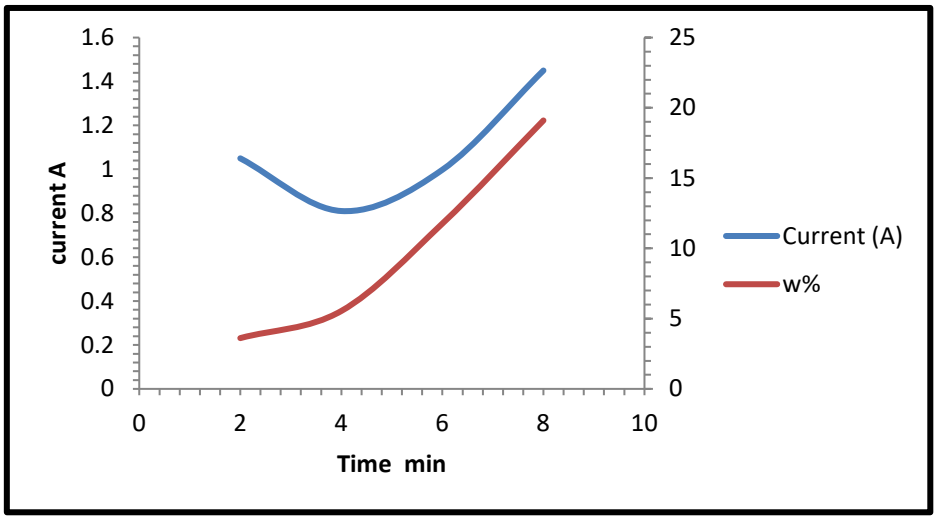

Fig. 12. Current (A) and weight loss percentage (%) versus different duration time for EP treatment of at 16 (V) BCC specimens

From the Figures 10-12 electro polish process at 8, 6 and 4 minutes are more effective for surface modification of HC, FCC and BCC of lattice specimens, sequentially. The shape of the curves explains the mechanism of EP treatment, where the initial decrease in current corresponds to removed balling influence and partially melted powder particles adhering to the surfaces on each side of the struts where increases the surface area of the electrode (lattice specimens) and the increased in current corresponds to the remove the oxide layer that forms during SLM, allowing the base alloy of the lattice specimens to be exposed to the polishing electrolyte. In HC lattice specimen, the amount of weight loss percentage (ΔW%) after 2 minutes of EP treatment is 1.625 %, after 4 minutes is 5.599 %, after 6 minutes is 6.612 %, and after 8 minutes is 8.693 %, and after 10 minutes is 13.352 %. In the HC specimens, Figure 13 are showed after 10 minutes of EP treatment the current and the weight loss ratio increased, and it observe small pits on the specimen surface, which in turn resulted in an increase in surface roughness and lower polishing quality and the lattice struts become thinner and a reduction in diameter of ~206.51 µm as in Figure 13.

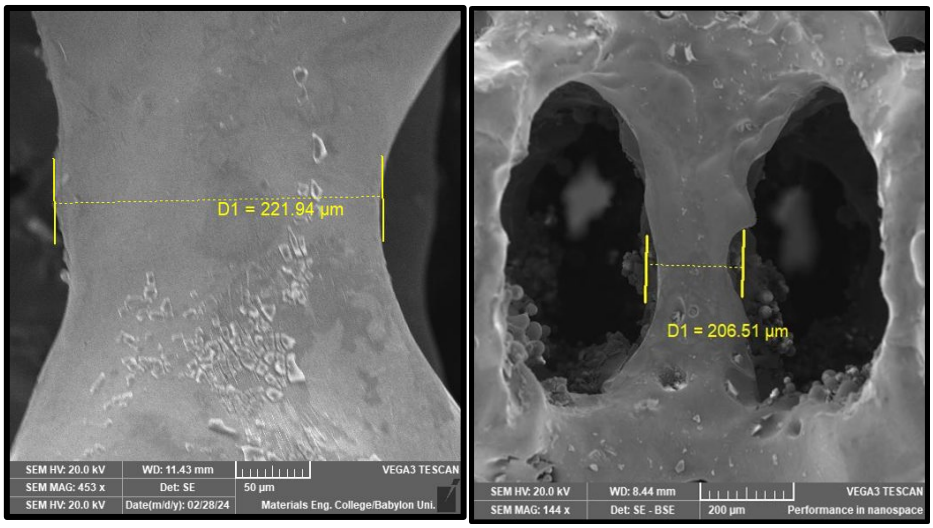

Fig. 13. SEM of HC lattice specimens after electro polishing for (a) 8 min and (b) 10 min

Damage and deterioration of the struts due to cracks make the lattice susceptible to pitting corrosion, which could further form internal cavities or holes that observed in Figure 14.

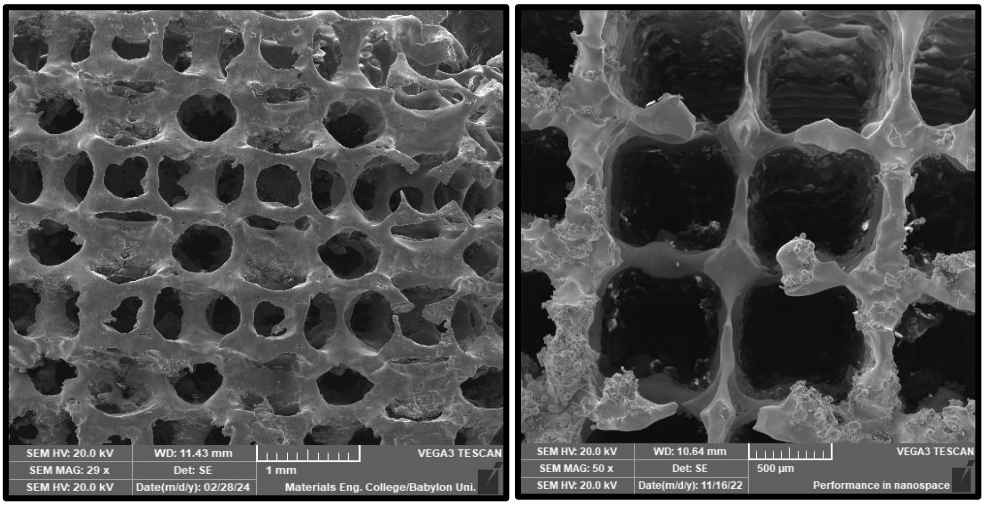

Fig. 14. Damage and deterioration of lattice specimens: (A)EP treatment of HC after 14 min, and (B) EP treatment of BCC after 10 min

4.3 Surface Roughness Analyses

During the EP treat meant of the HC,FCC and BCC lattice structures, electro polishing is showed selectively removing of material on surfaces, where resulting in up skin surfaces smoother than down skin surfaces due to the physics behind in the SLM process [40]. If the time increased in EP treatment observed the down skin surfaces are becoming smoother and with an increase in irregular and roughness of up skin facing surfaces with initial stair-stepping remaining on surface as in Figure 15 (A, B and C), therefore cannot the increase roughness improvement percentage magnitude between lattice specimens (as print) and after EP treatment of lattice specimens. Electro polish treatment conditions, weight loss % and surface roughness of the lattice specimens (HC, FCC and BCC) such as the root mean square deviation (Ra) and the max height of the profile (Rz) before and after electro polishing as shown in Table 3. The information about topography (Ra, Rq) of lattice structures specimens before and after EP treatment can be calculated from Figures 16-19.

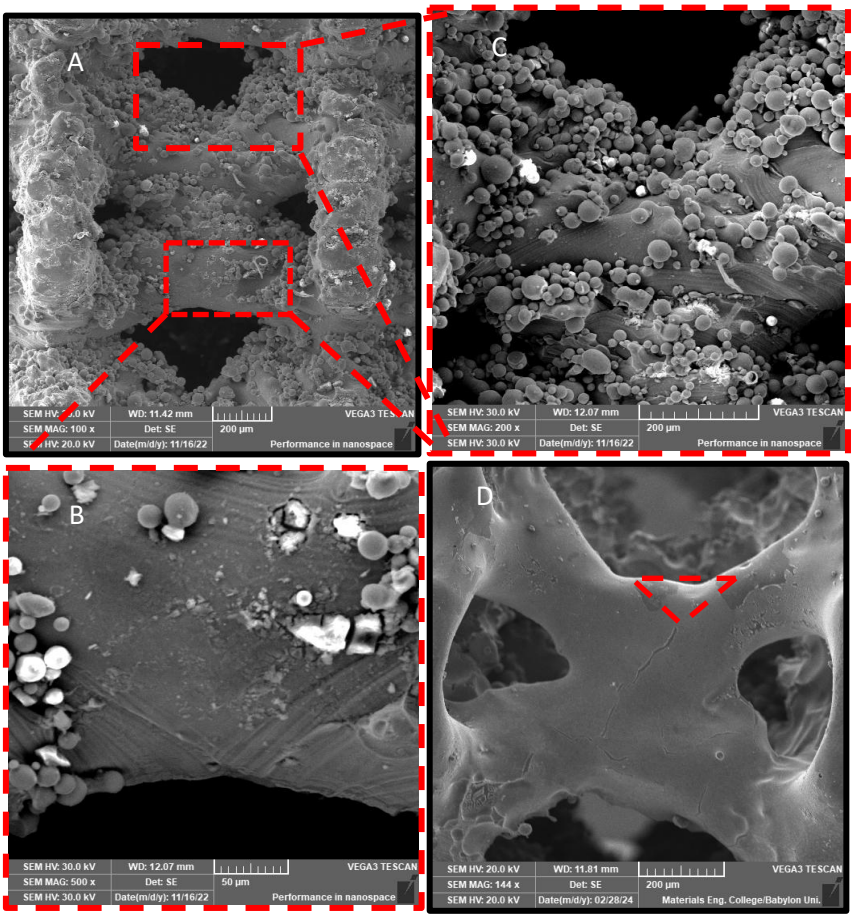

Fig. 15. SEM images showing skin and down skin surfaces for FCC lattice specimen

Table 3
Electro polish treatment conditions and Surface roughness of the lattice specimens before and after before and after electro polishing.

specimen	Before EP treatment		EP Time(min.)	Current (A)	Voltage (V)	Wight loss (%)	After EP treatment	
	Ra (µm)	Rz(µm)					Ra(µm)	Rz(µm)
HC	7.325	36.766	8	1.76	20	8.693	4.661	22.482
FCC	7.465	35.768	6	1.20	18	4.369	3.911	17.88
BCC	6.77	30.029	4	0.81	16	5.545	4.20	18.249

Additionally, there were also noticeably fewer foreign particles remaining on the surface of the lattice from the ultrasonic abrasive process.

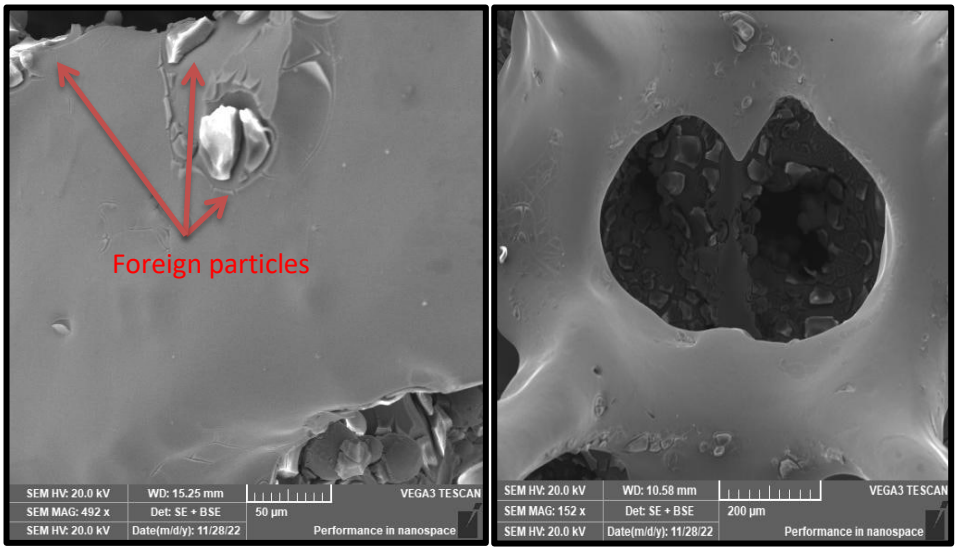

Fig. 16. SEM images showing few foreign particles remaining on the surface of the lattice HC lattice specimen

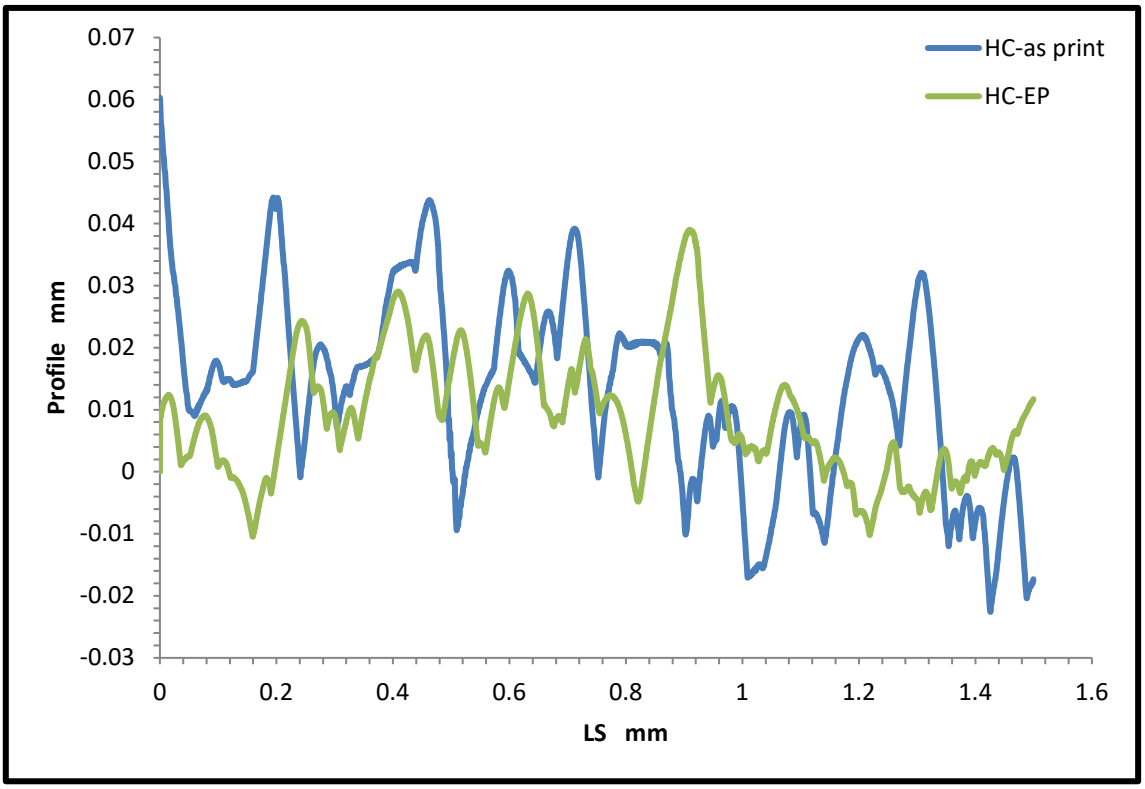

Fig. 17. Surface profile of HC lattice specimens before and after electro polishing

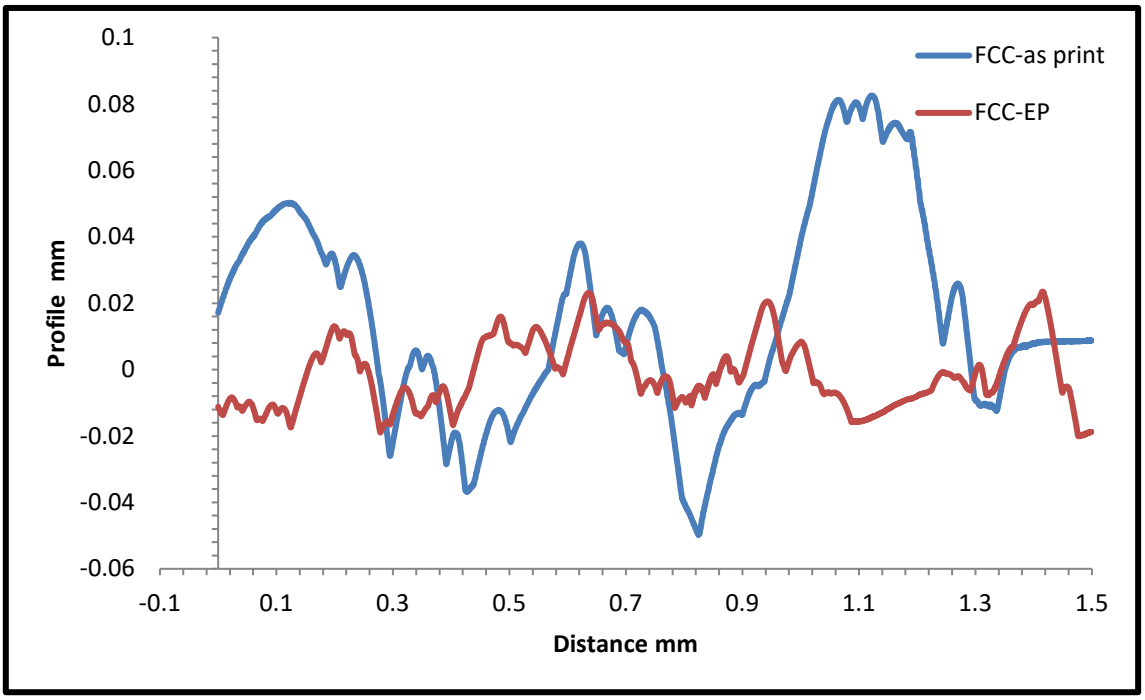

Fig. 18. Surface profile of FCC lattice specimens before and after electro polishing

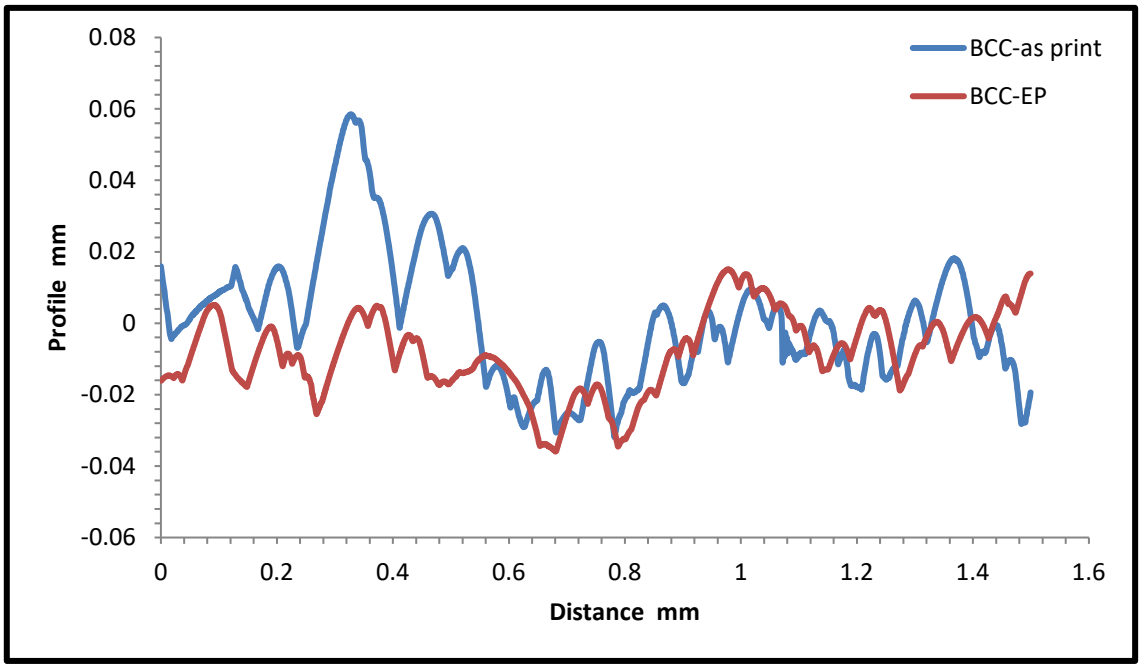

Fig. 19. Surface profile of BCC lattice specimens before and after electro polishing

4.4 Porosity Percentage Analyses

The porosity (%) of Ti6Al4V alloy lattice structure for 3D printing by SLM is an important parameter that must be carefully controlled to balance mechanical strength and biological performance [41]. After electro polishing treatment, the specimens showed an increase in the porosity percentage, where the porosity percentage of the Hexagonal cubic, Face center cubic, and body center cubic specimens are 60%, 65%, and 71%, respectively, with corresponding densities (g/cm3) of 1.7797, 1.5543, and 1.277. As a result of removing some defects associated with the building process, such as residual powder, ball influence and the attached partially melted particles.

It is important to mention that the porosity percentage of electro polish scaffolds are decrease about of (12–14) % compared of the Lattice structure design (HC, FCC and BCC) as shown in Figure 20.

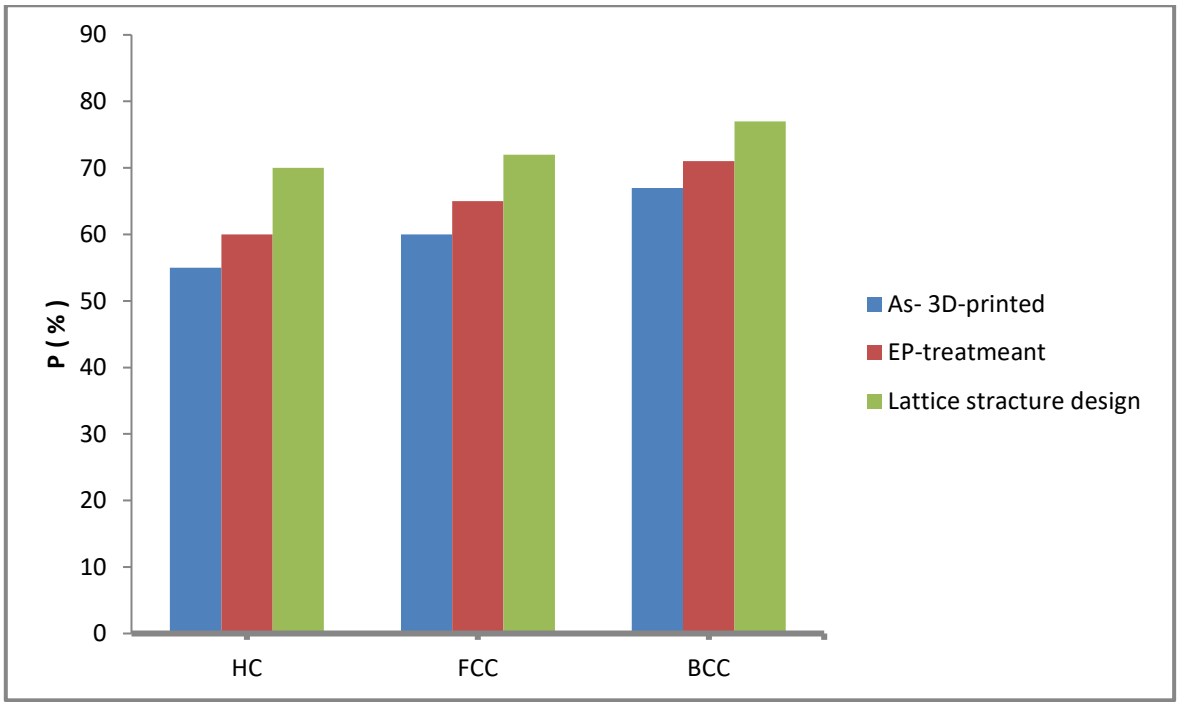

Fig. 20. Comparison of porosity (%) for lattice structures printed, electro-polished treat meant and design of lattice structures

4.5 Compression Teat Analyses

Figure 21 shows the findings of the stress-strain curves for the body-centered cubic, face-centered cubic, and hexagonal cubic lattice structures showed good agreement between the yield stress and modulus of Cortical bone in human bodies. The specimens exhibited a smooth transition from the elastic region to the plastic region [40]. The differences between the experimental findings and the theoretical predictions can be attributed to manufacturing and material defects, such as imperfect geometry, high surface roughness, micro porosity, and deviations of the strut axes from their nominal positions. It was observed that lattice structure samples (FCC, BCC, and HCP) exhibited a reduction in yield strength (MPa) and modulus of elasticity (GPa) by a percentage range of 7.5% to 9% after post-processing treatment. The findings in Table 4 show the Young's modulus, yield strength, and compare them with cortical bone for the tested specimens.

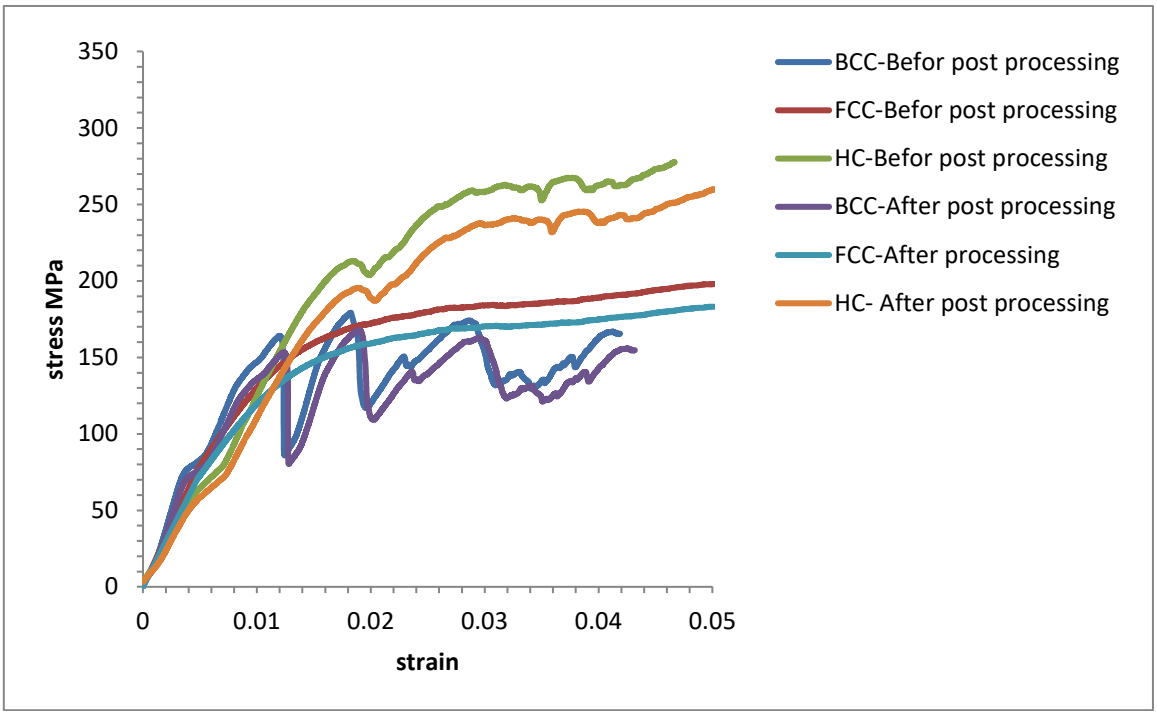

Fig. 21. stress –strain diagram by Compression teat for FCC, BCC and HC lattice structures

Table 4
Mechanical properties obtained from Stress strain findings and cortical bone under compression test

Lattice structures	Yield strength (MPa)		Modulus of elasticity (GPa)	
	Before-Treatment	After-Treatment	Before-Treatment	After- Treatment
BCC	144.34	134.44	14.159	13.859
FCC	155.137	143.637	13.55	12.75
HC	203.43	187.65	14.55	13.35
Cortical bone [42,43]	125-210		6-30	

5. Conclusion

In the present investigation, Ti6A4V lattice structures printed in three-dimensional through SLM were gained with surface morphology and mechanic features compatible and appropriate to act as scaffolds in human bodies.

The following are the key observations and inferences of this study:

i. It was probable to successfully print in three-dimensional Ti6Al4V thru SLM and surface treatment them to reduce the residual powder such as unmolten particles and loosely bound particles clusters by ultrasonic abrasive (SiC) flow and attached partially melted particles and balling influence by Electro polishing of different lattice structures.
ii. Total porosity situated between 60% and 71%. The root means square deviation (Ra) and the max height of the profile (Rz) after electro polishing are found between (3.91 - 4.661), and (17.88-22.482) µm. The magnitudes presented are appropriate for cellular proliferation and fluid transport if utilized as bone scaffolds on human body.
iii. Regarding mechanical behavior, elastic modulus is situated between 12.750 and 13.859 GPa. The yield strength between 134.44 and 187.65 MPa for different lattice structures. These findings are appropriate for scaffolds in human bone.

References

[1] Bandyopadhyay, Amit, Indranath Mitra, Stuart B. Goodman, Mukesh Kumar, and Susmita Bose. "Improving biocompatibility for next generation of metallic implants." *Progress in Materials Science* 133 (2023): 101053. https://doi.org/10.1016/j.pmatsci.2022.101053

[2] Hossain, Md Imam, Md Sakib Khan, Imrul Kayes Khan, Khan Rajib Hossain, Yanzhao He, and Xiaolong Wang. "TECHNOLOGY OF ADDITIVE MANUFACTURING: A COMPREHENSIVE REVIEW." *Kufa Journal of Engineering* 15, no. 1 (2024): 108-146.

[3] Alfaify, Abdullah, Mustafa Saleh, Fawaz M. Abdullah, and Abdulrahman M. Al-Ahmari. "Design for additive manufacturing: A systematic review." *Sustainability* 12, no. 19 (2020): 7936. https://doi.org/10.3390/su12197936

[4] Jiang, Shan, Dongliang Guo, Lei Zhang, Kan Li, Bo Song, and YongAn Huang. "Electropolishing-enhanced, high-precision 3D printing of metallic pentamode metamaterials." *Materials & Design* 223 (2022): 111211. https://doi.org/10.1016/j.matdes.2022.111211

[5] Hussein, Eman Yasir, Jassim M. Salman Al-Murshdy, Nabaa Sattar Radhi, and Zainab Al-Khafaji. "Surface Modification of Titanium Alloy by Titania/Silver Multilayers Coating for Biomedical Application." *Journal of Advanced Research in Micro and Nano Engineering* 20, no. 1 (2024): 66-78. https://doi.org/10.37934/armne.20.1.6678

[6] Pan, Chen, Yafeng Han, and Jiping Lu. "Design and optimization of lattice structures: A review." *Applied Sciences* 10, no. 18 (2020): 6374.. https://doi.org/10.3390/app10186374

[7] Ramaprasad, H., and B. Shreeprakash. "Review on Design and Additive Manufacturing of Cellular Lattice Structures By Extrusion Technologies." *Academic Journal of Manufacturing Engineering* 21, no. 3 (2023): 118–26.

[8] Al-Abayechi, Yasir, Yaser Alaiwi, and Zainab Al-Khafaji. "Exploration of key approaches to enhance evacuated tube solar collector efficiency." *Journal of Advanced Research in Numerical Heat Transfer* 19, no. 1 (2024): 1-14. https://doi.org/10.37934/arnht.19.1.114

[9] Fahad, Nesreen Dakhel, Nabaa Sattar Radhi, Zainab S. Al-Khafaji, and Abass Ali Diwan. "Surface modification of hybrid composite multilayers spin cold spraying for biomedical duplex stainless steel." *Heliyon* 9, no. 3 (2023). https://doi.org/10.1016/j.heliyon.2023.e14103

[10] Radhi, Nabaa S., and Z. A. I. N. A. B. Al-Khafaji. "Investigation biomedical corrosion of implant alloys in physiological environment." *Int J Mech Prod Eng Res Dev* 8, no. 4 (2018): 247-56. Doi: 10.24247/ijmperdaug201827.

[11] Al-Khafaji, Z., M. Kazem, N. Radhi, M. Falah, and Z. Hadi. "Reducing the Issues of Implements in the Human Body by Applying Hydroxyapatite (HAP) in Modern Biomedicine." *Material and Mechanical Engineering Technology* 64, no. 2 (2024). https://doi.org/10.52209/2706-977X

[12] Mobarak, Md Hosne, Md Aminul Islam, Nayem Hossain, Md Zobair Al Mahmud, Md Thohid Rayhan, Nushrat Jahan Nishi, and Mohammad Asaduzzaman Chowdhury. "Recent advances of additive manufacturing in implant fabrication–a review." *Applied Surface Science Advances* 18 (2023): 100462. https://doi.org/10.1016/j.apsadv.2023.100462

[13] Dong, Guoying, Yunlong Tang, and Yaoyao Fiona Zhao. "A survey of modeling of lattice structures fabricated by additive manufacturing." *Journal of Mechanical Design* 139, no. 10 (2017): 100906. https://doi.org/10.1115/1.4037305

[14] Chen, Jianyu, Zhiguang Zhang, Xianshuai Chen, Chunyu Zhang, Gong Zhang, and Zhewu Xu. "Design and manufacture of customized dental implants by using reverse engineering and selective laser melting technology." *The Journal of prosthetic dentistry* 112, no. 5 (2014): 1088-1095. https://doi.org/10.1016/j.prosdent.2014.04.026

[15] Choy, Wen Jie, Ralph J. Mobbs, Ben Wilcox, Steven Phan, Kevin Phan, and Chester E. Sutterlin III. "Reconstruction of thoracic spine using a personalized 3D-printed vertebral body in adolescent with T9 primary bone tumor." *World Neurosurgery* 105 (2017): 1032-e13. https://doi.org/10.1016/j.wneu.2017.05.133

[16] Chen, Xing, Jessy K. Possel, Catherine Wacongne, Anne F. Van Ham, P. Christiaan Klink, and Pieter R. Roelfsema. "3D printing and modelling of customized implants and surgical guides for non-human primates." *Journal of neuroscience methods* 286 (2017): 38-55. https://doi.org/10.1016/j.jneumeth.2017.05.013

[17] Arabnejad, Sajad, Burnett Johnston, Michael Tanzer, and Damiano Pasini. "Fully porous 3D printed titanium femoral stem to reduce stress-shielding following total hip arthroplasty." *Journal of Orthopaedic Research* 35, no. 8 (2017): 1774-1783. https://doi.org/10.1002/jor.23445

[18] Li, Ruidi, Jinhui Liu, Yusheng Shi, Li Wang, and Wei Jiang. "Balling behavior of stainless steel and nickel powder during selective laser melting process." *The International Journal of Advanced Manufacturing Technology* 59 (2012): 1025-1035. https://doi.org/10.1007/s00170-011-3566-1

[19] Kelly, Cambre N., Nathan T. Evans, Cameron W. Irvin, Savita C. Chapman, Ken Gall, and David L. Safranski. "The effect of surface topography and porosity on the tensile fatigue of 3D printed Ti-6Al-4V fabricated by selective

laser melting." *Materials Science and Engineering: C* 98 (2019): 726-736. https://doi.org/10.1016/j.msec.2019.01.024

[20] Minasyan, T., S. Aydinyan, E. Toyserkani, and I. Hussainova. "Parametric Study on In Situ Laser Powder Bed Fusion of Mo (Si1− x, Alx) 2." *Materials* 13, no. 21 (2020): 4849. https://doi.org/10.3390/ma13214849

[21] Tang, Ming, P. Chris Pistorius, and Jack L. Beuth. "Prediction of lack-of-fusion porosity for powder bed fusion." *Additive Manufacturing* 14 (2017): 39-48. https://doi.org/10.1016/j.addma.2016.12.001

[22] Olsson, Rickard, John Powell, Anders Palmquist, Rickard Brånemark, Jan Frostevarg, and Alexander FH Kaplan. "Formation of osseointegrating (bone integrating) surfaces on titanium by laser irradiation." *Journal of Laser Applications* 31, no. 2 (2019). https://doi.org/10.2351/1.5096075

[23] Davoodi, Elham, Hossein Montazerian, Anooshe Sadat Mirhakimi, Masoud Zhianmanesh, Osezua Ibhadode, Shahriar Imani Shahabad, Reza Esmaeilizadeh et al. "Additively manufactured metallic biomaterials." *Bioactive materials* 15 (2022): 214-249. https://doi.org/10.1016/j.bioactmat.2021.12.027

[24] Al-Maharma, Ahmad Y., Sandeep P. Patil, and Bernd Markert. "Effects of porosity on the mechanical properties of additively manufactured components: a critical review." *Materials Research Express* 7, no. 12 (2020): 122001. https://doi.org/10.1088/2053-1591/abcc5d

[25] Jiang, Panwei, Mustafa Rifat, and Saurabh Basu. "Impact of surface roughness and porosity on lattice structures fabricated by additive manufacturing-A computational study." *Procedia Manufacturing* 48 (2020): 781-789. https://doi.org/10.1016/j.promfg.2020.05.114

[26] Kantaros, Antreas, Theodore Ganetsos, Florian Ion Tiberiu Petrescu, Liviu Marian Ungureanu, and Iulian Sorin Munteanu. "Post-Production Finishing Processes Utilized in 3D Printing Technologies." *Processes* 12, no. 3 (2024): 595. https://doi.org/10.3390/pr12030595

[27] Ferchow, Julian, Urs Hofmann, and Mirko Meboldt. "Enabling electropolishing of complex selective laser melting structures." *Procedia CIRP* 91 (2020): 472-477. https://doi.org/10.1016/j.procir.2020.02.201

[28] Łyczkowska-Widłak, Edyta, Paweł Lochyński, and Ginter Nawrat. "Electrochemical polishing of austenitic stainless steels." *Materials* 13, no. 11 (2020): 2557. https://doi.org/10.3390/ma13112557

[29] Tyagi, Pawan, Denikka Brent, Tyler Saunders, Tobias Goulet, Christopher Riso, Kate Klein, and Francisco Garcia Moreno. "Roughness reduction of additively manufactured steel by electropolishing." *The International Journal of Advanced Manufacturing Technology* 106 (2020): 1337-1344. https://doi.org/10.1007/s00170-019-04720-z

[30] Han, Wei, and Fengzhou Fang. "Fundamental aspects and recent developments in electropolishing." *International Journal of Machine Tools and Manufacture* 139 (2019): 1-23. https://doi.org/10.1016/j.ijmachtools.2019.01.001

[31] Kim, Uk Su, and Jeong Woo Park. "High-quality surface finishing of industrial three-dimensional metal additive manufacturing using electrochemical polishing." *International Journal of Precision Engineering and Manufacturing-Green Technology* 6 (2019): 11-21. https://doi.org/10.1007/s40684-019-00019-2

[32] Yang, Li, Hengfeng Gu, and Austin Lassell. "Surface treatment of Ti6al4V parts made by powder bed fusion additive manufacturing processes using electropolishing." (2014).

[33] Sattar, Sabaa, Yaser Alaiwi, Nabaa Sattar Radhi, and Zainab Al-Khafaji. "NUMERICAL SIMULATION FOR EFFECT OF COMPOSITE COATING (TIO2+ SIO2) THICKNESS ON STEAM TURBINE BLADES THERMAL AND STRESS DISTRIBUTION." *Academic Journal of Manufacturing Engineering* 21, no. 4 (2023).

[34] Dawood, Nawal Mohammed, Nabaa S. Radhi, and Zainab S. Al-Khafaji. "Investigation corrosion and wear behavior of Nickel-Nano silicon carbide on stainless steel 316L." In *Materials Science Forum*, vol. 1002, pp. 33-43. Trans Tech Publications Ltd, 2020. https://doi.org/10.4028/www.scientific.net/MSF.1002.33

[35] Jasim, Ahlam Hamid, Nabaa S. Radhi, Noor Emad Kareem, Zainab S. Al-Khafaji, and Mayadah Falah. "Identification and investigation of corrosion behavior of electroless composite coating on steel substrate." *Open Engineering* 13, no. 1 (2023): 20220472. https://doi.org/10.1515/eng-2022-0472

[36] Radhi, Nabaa Sattar, Zainab Al-Khafaji, Basim M. Mareai, Sabaa Radhi, and Ayam M. Alsaegh. "Reducing oil pipes corrosion by (ZN-NI) alloy coating on low carbon steel substrate by sustainable process." *Journal of Engineering Science and Technology* 18, no. 3 (2023): 1624-1638.

[37] Sattar, Sabaa, Yaser Alaiwi, Nabaa Sattar Radhi, Zainab Al-Khafaji, Osamah Al-Hashimi, Hassan Alzahrani, and Zaher Mundher Yaseen. "Corrosion reduction in steam turbine blades using nano-composite coating." *Journal of King Saud University-Science* 35, no. 8 (2023): 102861. https://doi.org/10.1016/j.jksus.2023.102861

[38] Abed Janabi, Zainab Makki, Haydar Shamkhi Jaber Alsalami, Zainab Sattar Al-Khafaji, and Safa A. Hussien. "Increasing of the corrosion resistance by preparing the trivalent nickel complex." *Egyptian Journal of Chemistry* 65, no. 6 (2022): 193-198. DOI: 10.21608/ejchem.2021.100733.4683

[39] Ahmed, Nissar, Imad Barsoum, G. Haidemenopoulos, and RK Abu Al-Rub. "Process parameter selection and optimization of laser powder bed fusion for 316L stainless steel: A review." *Journal of Manufacturing Processes* 75 (2022): 415-434. https://doi.org/10.1016/j.jmapro.2021.12.064

[40] Fiume, Elisa, Jacopo Barberi, Enrica Verné, and Francesco Baino. "Bioactive glasses: from parent 45S5

composition to scaffold-assisted tissue-healing therapies." *Journal of functional biomaterials* 9, no. 1 (2018): 24. https://doi.org/10.3390/jfb9010024

[41] Metelkova, Jitka, Daniel Ordnung, Yannis Kinds, and Brecht Van Hooreweder. "Novel strategy for quality improvement of up-facing inclined surfaces of LPBF parts by combining laser-induced shock waves and in situ laser remelting." *Journal of Materials Processing Technology* 290 (2021): 116981. https://doi.org/10.1016/j.jmatprotec.2020.116981

[42] Mullen, Lewis, Robin C. Stamp, Wesley K. Brooks, Eric Jones, and Christopher J. Sutcliffe. "Selective Laser Melting: A regular unit cell approach for the manufacture of porous, titanium, bone in-growth constructs, suitable for orthopedic applications." *Journal of Biomedical Materials Research Part B: Applied Biomaterials: An Official Journal of The Society for Biomaterials, The Japanese Society for Biomaterials, and The Australian Society for Biomaterials and the Korean Society for Biomaterials* 89, no. 2 (2009): 325-334. https://doi.org/10.1002/jbm.b.31219

[43] Arabnejad, Sajad, R. Burnett Johnston, Jenny Ann Pura, Baljinder Singh, Michael Tanzer, and Damiano Pasini. "High-strength porous biomaterials for bone replacement: A strategy to assess the interplay between cell morphology, mechanical properties, bone ingrowth and manufacturing constraints." *Acta biomaterialia* 30 (2016): 345-356. https://doi.org/10.1016/j.actbio.2015.10.048